Pharmacokinetics and Tissue Disposition of Indole-3-carbinol and Its Acid Condensation Products after Oral Administration to Mice

Mark J. Anderton,[1] Margaret M. Manson,[1] Richard D. Verschoyle,[1] Andreas Gescher,[1] John H. Lamb,[1] Peter B. Farmer,[1] William P. Steward,[1] and Marion L. Williams[2]

[1]Cancer Biomarkers and Prevention Group, Departments of Biochemistry and Cancer Studies and Molecular Medicine, University of Leicester, Leicester, United Kingdom, and [2]National Institute on Aging, Gerontology Research Center, Baltimore, Maryland

ABSTRACT

Indole-3-carbinol (I3C) and 3,3′-diindolylmethane (DIM) are promising cancer chemopreventive agents in rodent models, but there is a paucity of data on their pharmacokinetics and tissue disposition. The disposition of I3C and its acid condensation products, DIM, [2-(indol-3-ylmethyl)-indol-3-yl]indol-3-ylmethane (LTr_1), indolo[3,2b]carbazole (ICZ) and 1-(3-hydroxymethyl)-indolyl-3-indolylmethane (HI-IM) was studied, after oral administration of I3C (250 mg/kg) to female CD-1 mice. Blood, liver, kidney, lung, heart, and brain were collected between 0.25 and 24 h after administration and the plasma and tissue concentrations of I3C and its derivatives determined by high-performance liquid chromotography. I3C was rapidly absorbed, distributed, and eliminated from plasma and tissues, falling below the limit of detection by 1 h. Highest concentrations of I3C were detected in the liver where levels were approximately 6-fold higher than those in the plasma. Levels of DIM, LTr_1, and HI-IM were much lower, although they persisted in plasma and tissues for considerably longer. DIM and HI-IM were still present in the liver 24 h after I3C administration. Tissue levels of DIM and LTr_1 were found to be in equilibrium with plasma at almost every time point measured. In addition to acid condensation products of I3C, a major oxidative metabolite (indole-3-carboxylic acid) and a minor oxidative metabolite (indole-3-carboxaldehyde) were detected in plasma of mice after oral administration of I3C. ICZ was also tentatively identified in the liver of these mice. This study shows for the first time that, after oral administration to mice, I3C, in addition to its acid condensation products, is absorbed from the gut and distributed systemically into a number of well-perfused tissues, thus allowing the possibility for some pharmacological activity of the parent compound *in vivo*.

INTRODUCTION

Indole-3-carbinol (I3C) is a naturally occurring hydrolysis product of glucobrassicin found in vegetables of the *Cruciferae* family such as broccoli, brussels sprouts, and cauliflower. Epidemiological studies suggest high dietary intake of cruciferous vegetables is associated with lower cancer risk (1), and it is possible that the chemopreventive properties are in part attributable to I3C (2). Indeed, it has been demonstrated that I3C is an effective chemopreventive agent in rodents, active against a number of carcinogen-induced and spontaneous tumors in multiple tissues, including mammary gland (3, 4), liver (5), lung (6), tongue and nasal mucosa (7), and endometrium (8).

One of the primary mechanisms by which I3C prevents tumorigenesis is by selective beneficial alteration of Phase I and Phase II carcinogen-metabolising enzymes (9, 10). I3C has also been shown to have antiestrogenic activity that is proposed to account for its protective and antiproliferative effects on estrogen-responsive tissues. I3C induces estradiol 2-hydroxylase, thus increasing the metabolic ratio of 2-hydroxyestrone:16α-hydroxyestrone in rodents (3) and humans (11). In addition, I3C can induce a G_1 cell cycle arrest (12), as well as apoptosis and inhibition of Akt phosphorylation in human breast (13) and prostate (14, 15) tumor cells lines.

I3C is susceptible to oligomerization under acidic conditions approximating those in gastric juice (16) and thus, after ingestion, is converted into several condensation products. It has been suggested that the observed biological activity may be attributable mainly to the acid condensation products, in particular, 3,3′-diindolylmethane (DIM; Fig. 1). [2-(Indol-3-ylmethyl)-indol-3-yl]indol-3-ylmethane (LTr_1; Fig. 1), indolo[3,2b]carbazole (ICZ; Fig. 1) and 5,6,11,12,17,18-hexahydrocyclonona[1,2-b:4,5-b′:7,8-b″]tri-indole (cyclic trimer) have also all been identified in rodents after oral administration of I3C (17, 18). Cyclic trimer, ICZ, and LTr_1 have been shown to exhibit biological activity (19–21), and in particular, DIM has shown promising cancer chemopreventive properties *in vitro* (22) and *in vivo* (23).

Despite the accumulating knowledge regarding mechanisms responsible for the chemopreventive and antitumor properties of I3C, there have been relatively few studies determining the disposition of I3C in rodents or humans. In fact this issue was identified recently by an IARC Working Group (24) as an area in which research is badly needed. The disposition and excretion of radiolabeled I3C has been determined in male Fischer rats (18) and rainbow trout (25). DIM has also been quantified in human plasma after I3C administration (26).

Because of the paucity of detailed information on the

Received 1/27/04; revised 4/30/04; accepted 5/6/04.
Grant support: This research was supported by the Medical Research Council, United Kingdom (Grants GO100872, GO100873, and GO100874)
The costs of publication of this article were defrayed in part by the payment of page charges. This article must therefore be hereby marked *advertisement* in accordance with 18 U.S.C. Section 1734 solely to indicate this fact.
Requests for reprints: Margaret M. Manson. Biocentre, University Road, Leicester, LE1 7RH, United Kingdom. Phone: 44-116-223-1822; Fax: 44-116-223-1840; E-mail: mmm2@le.ac.uk.

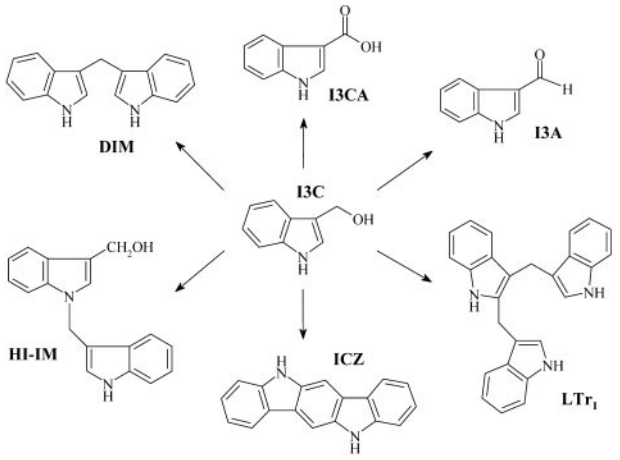

Fig. 1 Structure of I3C and its metabonates found in plasma and/or tissues of mice that received I3C by the oral route. *I3C*, indole-3-carbinol; *DIM*, 3,3′-diindolylmethane; *I3CA*, indole-3-carboxylic acid; *I3A*, indole-3-carboxaldehyde; *LTr$_1$*, linear trimer, [2-(indol-3-yl-methyl)-indol-3-yl]indol-3-ylmethane; *HI-IM*, [1-(3-hydroxymethyl)-indolyl-3-indolylmethane]; *ICZ*, indolo [3,2b]carbazole.

disposition of I3C in the intact organism, a recently developed high-performance liquid chromatography (HPLC) method was used for the analysis of I3C and its acid condensation products *in vivo* (17), with the aim of studying in detail the systemic absorption and tissue distribution in mice receiving I3C via the oral route.

MATERIALS AND METHODS

Chemicals. I3C, indole-3-carboxylic acid (I3CA), indole-3-carboxaldehyde (I3A), and the internal standard, 4-methoxy-indole, were purchased from Sigma-Aldrich Chemical Company (Poole, Dorset, United Kingdom). DIM was purchased from LKT Laboratories Inc. (St. Paul, MN). ICZ and LTr$_1$ were prepared in this laboratory to 97% purity according to methods described previously (17, 27). Acetonitrile and *t*-butyl methyl ether (both HPLC grade) and HEPES sodium salt were purchased from Sigma-Aldrich Chemical Company. All other solvents were HPLC or analytical grade Fisher Scientific (Loughborough, Leicestershire, United Kingdom). Water used in the preparation of all reagents and mobile phase was prepared by an ultrapure water system (ELGA, Bucks, United Kingdom).

Treatments. Female CD-1 mice (25–31 g), obtained from Harlan United Kingdom (Bicester, United Kingdom) were used under license from the Home Office and after approval by the University of Leicester Ethical Committee for Animal Experimentation. During the acclimatization period (1 week), they were housed in Moredun Isolators (Moredun Animal Health, Edinburgh, United Kingdom) under negative pressure, with a 12-h light-dark cycle, a temperature range of 20–23°C and 40–60% humidity. The mice were provided with pellet RM1 diet (Special Diets Services, Witham, United Kingdom) and water *ad libitum* before and during the experiment. On the dosing day, mice were removed from isolators and gavaged with I3C (250 mg/kg) as a suspension in corn oil (10 ml corn oil/kg body weight). Blood samples were collected by cardiac exsanguination under halothane anesthesia at 0.25, 0.5, 0.75, 1, 2, 4, 6, and 24 h after dosing. Four mice were used for each time point. Control animals received corn oil (10 ml/kg) and were culled 0.5 h after dosing. Each blood sample was collected in a heparinized tube. The plasma fraction was immediately separated by centrifugation (10,000 × g, 5 min) and stored at −80°C until analysis. After exsanguination, liver, kidney, lung, heart, and brain were immediately removed, wrapped in aluminum foil, snap frozen in liquid nitrogen, and stored frozen at −80°C until analysis.

Plasma Extraction and Analysis. Plasma concentrations of I3C, DIM, and LTr$_1$ were determined using a HPLC method described previously (17). In brief, the internal standard (4-methoxy-indole; 2.5 μl of a 0.4 mg/ml solution) was added to plasma samples (250 μl). The samples were vortex-mixed and equilibrated at room temperature for 30 min. Samples were extracted twice with *t*-butyl methyl ether (750 μl), involving 2-min vortexing on each occasion. Subsequent to each extraction, the organic and aqueous layers were separated by centrifugation (2800 × g, 10 min) and the organic (top) layers transferred to a fresh 4-ml tube. The top layers of each extraction were combined, and the *t*-butyl methyl ether evaporated to dryness in the presence of 15 μl of DMSO. The extracted sample in DMSO was then diluted using acetonitrile/50 mM HEPES buffer (pH 7.4; 40:60 v/v; 135 μl) and transferred to a glass vial insert for analysis by HPLC. Concentrations of I3C, DIM, and LTr$_1$ in experimental samples were determined by comparison of the peak area ratio of the analyte and internal standard against calibration curves prepared by spiking blank plasma from control mice with a known amount of stock solution. Calibration samples were extracted and analyzed in the same way as described previously for experimental plasma samples.

To estimate concentrations of I3CA in plasma, calibration curves were prepared and concentrations determined using the internal standard method, as described previously. This produced linear calibration curves ($r^2 > 0.99$) in the range investigated (0.1–15 μg/ml). 1-(3-Hydroxymethyl)-indolyl-3-indolylmethane (HI-IM) plasma concentrations were estimated using calibration curves prepared for DIM.

Tissue Extraction and Analysis. Each tissue was thawed, rinsed with ice-cold saline, blotted dry, weighed, and homogenized (1:1, w/v) in 50 mM HEPES buffer (pH 7.4) using a Ystral X 10/20 homogenizer (D-79282 Ballrechten-Dottingen, Germany). Aliquots of homogenates (250 μl) were transferred into clean 4-ml tubes, with the exception of heart, where 200 μl were used because of the small amount of tissue available. 4-Methoxy-indole (2.5 μl of 0.4 mg/ml) was added to the homogenate as internal standard. Samples were equilibrated on ice for 30 min. Acetonitrile (750 μl) was added to each sample and vortex-mixed for 2 min. Samples were then stored on ice for 5 min before being vortex-mixed again for a further 2 min. The tissue and solvent were separated by centrifugation (2800 × g, 10 min) and the solvent transferred to a fresh tube. The acetonitrile/water mixture was evaporated to dryness at room temperature in the presence of 15 μl of DMSO under a stream of nitrogen gas. The residue was resuspended in 135 μl of acetonitrile/50 mM HEPES buffer (pH 7.4; 40/60 v/v) and transferred to a clean 0.5-ml Eppendorf tube. Turbidity was removed by

Table 1 Concentration of I3C in plasma and tissues of female CD-1 mice that received an oral dose of I3C (250 mg/kg) by the oral route

	I3C concentration (μg/ml or μg/g tissue)					
Time (h)	Plasma	Liver	Kidney	Lung	Heart	Brain
0.25	4.13 ± 1.35	24.53 ± 5.48	16.95 ± 10.62	5.27 ± 2.24	5.27 ± 1.18	2.74 ± 0.89
0.5	2.21 ± 0.20	2.60 ± 0.39	3.73 ± 0.41	2.07 ± 1.25	2.84 ± 1.17	2.10 ± 0.22
0.75	0.12 ± 0.05	0.17 ± 0.13	0.35 ± 0.18	0.52 ± 0.43	0.56 ± 0.29	nd
1	nd	nd	nd	nd	nd	nd

NOTE. Results are expressed as mean ± SD of four animals.

Abbreviations: I3C, indole-3-carbinol; nd, not detected or the observed concentration was below the limit of quantification of the analytical method (0.05 μg/mL plasma, 0.1 μg/g tissue).

centrifugation (10,000 × *g*, 5 min) and the supernatant transferred to a glass vial insert before analysis by HPLC as described below.

Concentrations in experimental samples were determined by an internal standard method using calibration curves that were prepared using tissues from control mice. Calibration curves for I3C, DIM, and LTr_1 were prepared for lung, heart, brain, kidney, and liver between the range 0.1–30 μg/g. Concentrations of HI-IM in tissues were estimated using calibration curves for the structurally related DIM. ICZ was quantified in liver samples using a calibration curve prepared from 0.3–75 ng/g, using an external standard. This method was found to be more accurate for quantification of ICZ in plasma (17). The calibration curves for each compound in every tissue were linear ($r^2 > 0.99$) in the range investigated. The extraction efficiency of I3C, DIM, LTr_1, and ICZ was determined by comparison of the slope of a calibration curve prepared in mobile phase with a calibration curve for the same concentrations extracted from each specific tissue. Using this method, the extraction efficiencies of I3C, DIM, LTr_1, and ICZ were ≥69% and the internal standard ≥70% for all of the sampled tissues. The extraction methods were validated for analysis of liver, where the precision (expressed as coefficient of variation) was in the range of 5.2–10.2%. Accuracy values ranged from 91.2% to 108.4% for two quality control samples containing I3C, DIM, LTr_1, and ICZ.

Liquid Chromatography. HPLC analysis of plasma and tissue samples was performed on a Varian Prostar HPLC system (Varian Ltd., Surrey, United Kingdom). The system consisted of a 230 pump, 410 autosampler, 310 UV detector, and 363 fluorescence detector. The extracted standard/sample (50 μl) was injected onto the HPLC system. Chromatography was achieved using a Waters Symmetry RP 18 (4.6 × 50 mm, 5 μm) column (Hertford, United Kingdom) in tandem with a Thermoquest BDS C18 (250 × 4.6 mm, 5 μm) column (Runcorn, United Kingdom) and a Phenomenex C_{18} octadecyl silane (4 × 3 mm) guard column (Cheshire, United Kingdom). The mobile phase consisted of water (A) and acetonitrile (B). The gradient was as follows: 15% B to 60% B from 0 to 20 min; linear gradient to 65% B from 20 to 40 min; linear gradient to 85% B from 40 to 65 min, then re-equilibration to 15% B for 5 min. Total run time was 70 min, and the flow rate was 1 ml/min. Separation was carried out at room temperature. I3C, DIM, LTr_1, HI-IM, and I3CA were quantified by UV detection at 280 nm, whereas ICZ was quantified using fluorescence detection at 335:415 nm (ex./em.).

Identification of Metabonates of I3C. The acid condensation products and oxidative metabolites of I3C were identified by mass spectrometry of the peak of interest from the plasma and tissues. All samples were evaporated to dryness and resuspended in acetonitrile before analysis. If material from a single fraction did not provide the sensitivity required for characterization of the peak of interest, then a number of HPLC fractions were combined. Electron ionization spectra were obtained via direct insertion probe technique using a VG 70-SEQ mass spectrometer (Micromass, Manchester, United Kingdom). The conditions used were 70 eV electron energy, 200 μA trap current, and a source temperature of 250°C.

Statistical Analysis. Comparison of tissue and plasma concentrations and tissue-to-plasma ratios were performed using ANOVA and Tukey's multiple comparison post hoc test.

RESULTS

Plasma Levels and Tissue Distribution of I3C. After oral administration of I3C (250 mg/kg) to mice, the compound was rapidly absorbed and had already reached an apparent peak concentration of 4.1 μg/ml at the earliest sampling time point of 15 min after dose (Table 1). However, concentrations fell below the limit of detection within the 1st h after dosing, indicating rapid clearance.

I3C was rapidly and extensively distributed into all sampled tissues, with highest concentrations in the liver (Table 1). Peak levels here were significantly higher than in plasma and all of the other sampled tissues ($P < 0.001$), with the exception of kidney ($P > 0.05$). Similarly, peak kidney concentrations were significantly higher than levels in plasma, lung, heart, and brain ($P < 0.05$), which were not significantly different from one another.

Plasma Levels and Tissue Distribution of DIM and LTr_1. DIM and LTr_1 were detected in plasma and tissues after I3C administration (Fig. 2). DIM was detected in plasma at 15 min and was still quantifiable after 6 h, whereas LTr_1 was not detected in plasma until 1 h after dosing, and levels were still increasing at the last measurable time point of 6 h (Fig. 3). DIM appeared to reach its peak at 2 h after I3C dosing. The peak plasma concentrations of DIM and LTr_1 were approximately one sixth and one tenth that of I3C, although detectable levels persisted for much longer than their precursor (Table 1; Fig. 3).

DIM and LTr_1 were distributed to all tissues examined, with highest concentrations of both compounds in liver (Fig. 3). Tissue profiles were similar to those observed in plasma, sug-

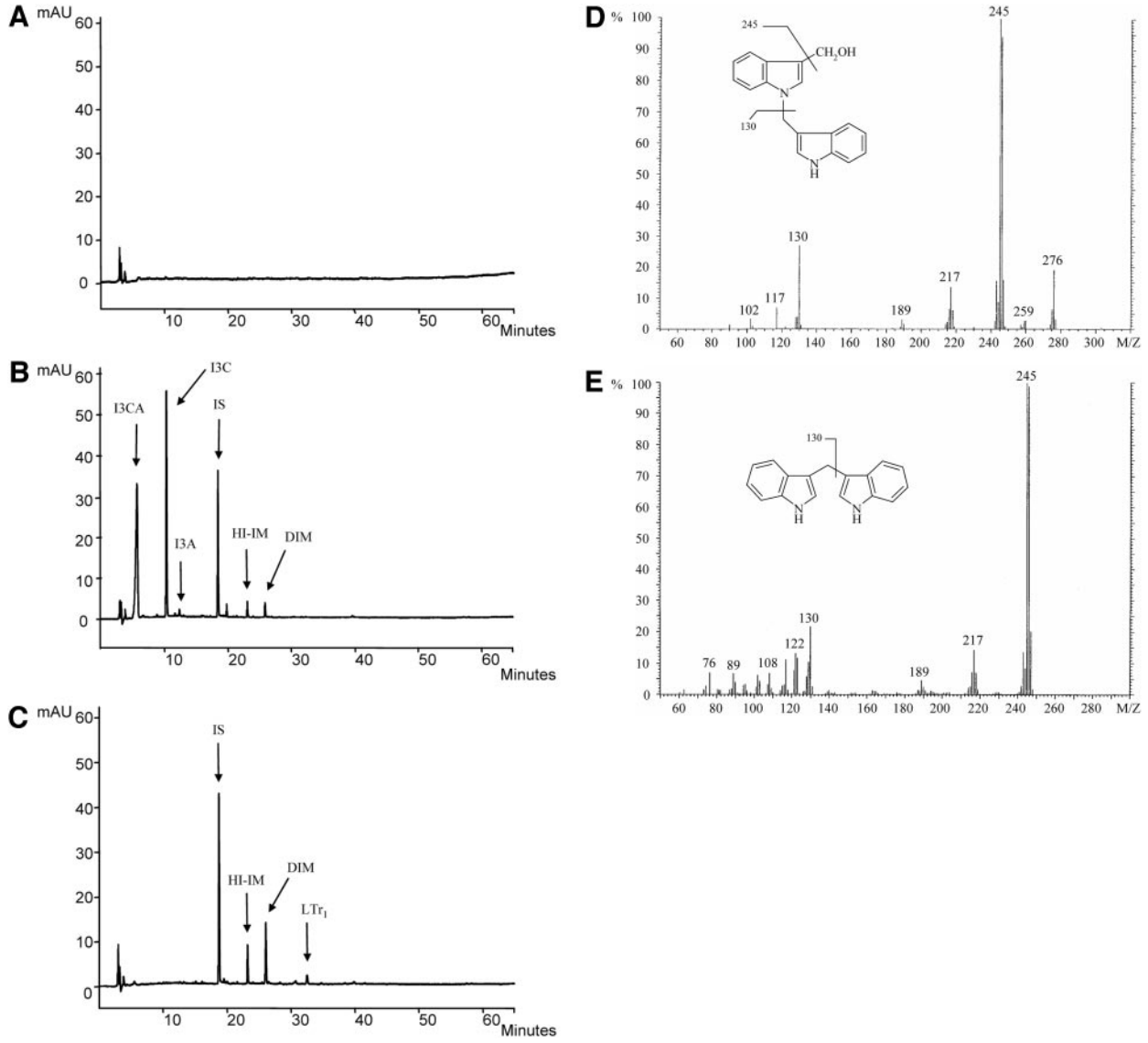

Fig. 2 High-performance liquid chromatography chromatograms of mouse plasma samples (*A*) after administration of carrier solvent or (*B*) 15 min after I3C (250 mg/kg), and (*C*) 1 h after I3C (250 mg/kg). Peaks are indicated as I3C, DIM, I3CA, I3A, LTr_1, HI-IM, and IS. Mass spectra obtained by electron ionization for (*D*) HI-IM and (*E*) DIM. *I3C*, indole-3-carbinol; *DIM*, 3,3′-diindolylmethane; *I3CA*, indole-3-carboxylic acid; *I3A*, indole-3-carboxaldehyde; *LTr_1*, linear trimer, [2-(indol-3-ylmethyl)-indol-3-yl]indol-3-ylmethane; *HI-IM*, [1-(3-hydroxymethyl)-indolyl-3-indolylmethane]; *IS*, 4-methoxy-indole.

gesting that DIM and LTr_1 were in equilibrium with the plasma. To test this hypothesis, mean tissue-to-plasma ratios for DIM (0.25–6 h) and LTr_1 (liver, 1–6 h; other tissues, 2–6 h) for each mouse at every time point were calculated (Table 2).

Generally, DIM exhibited similar tissue-to-plasma ratios at all time points, suggesting that distribution equilibrium had been rapidly achieved between plasma and all of the sampled tissues (Table 2; Fig. 4). Average tissue-to-plasma ratios over the full sampling time range are shown in Fig. 4. DIM ratios were ranked in the order: liver $\ggg$ kidney $\gg$ brain $\approx$ lung $\approx$ heart.

Once LTr_1 reached detectable levels, this compound also exhibited similar tissue-to-plasma ratios at all points of sampling, suggesting that distribution equilibrium was eventually achieved and maintained (Table 2; Fig. 4). Average tissue-to-plasma ratios of LTr_1 can be ranked in the following order: liver $\gg$ kidney $\approx$ lung $\approx$ heart $\gg$ brain (Fig. 4).

Plasma Levels and Tissue Distribution of HI-IM. After HPLC analysis of plasma and tissue samples from mice that had received I3C, an additional peak with a retention time of 23.2 min was detected (Fig. 2). The identity of this peak was confirmed by mass spectrometry to be HI-IM (Fig. 2). This product was identified previously, after oral administration of I3C to rats, by Stressor *et al.* (18). An HPLC standard for HI-IM was not available, but assuming HI-IM had a similar extraction efficiency and UV sensitivity to its structurally related compound DIM, estimation of the plasma and tissue concentrations

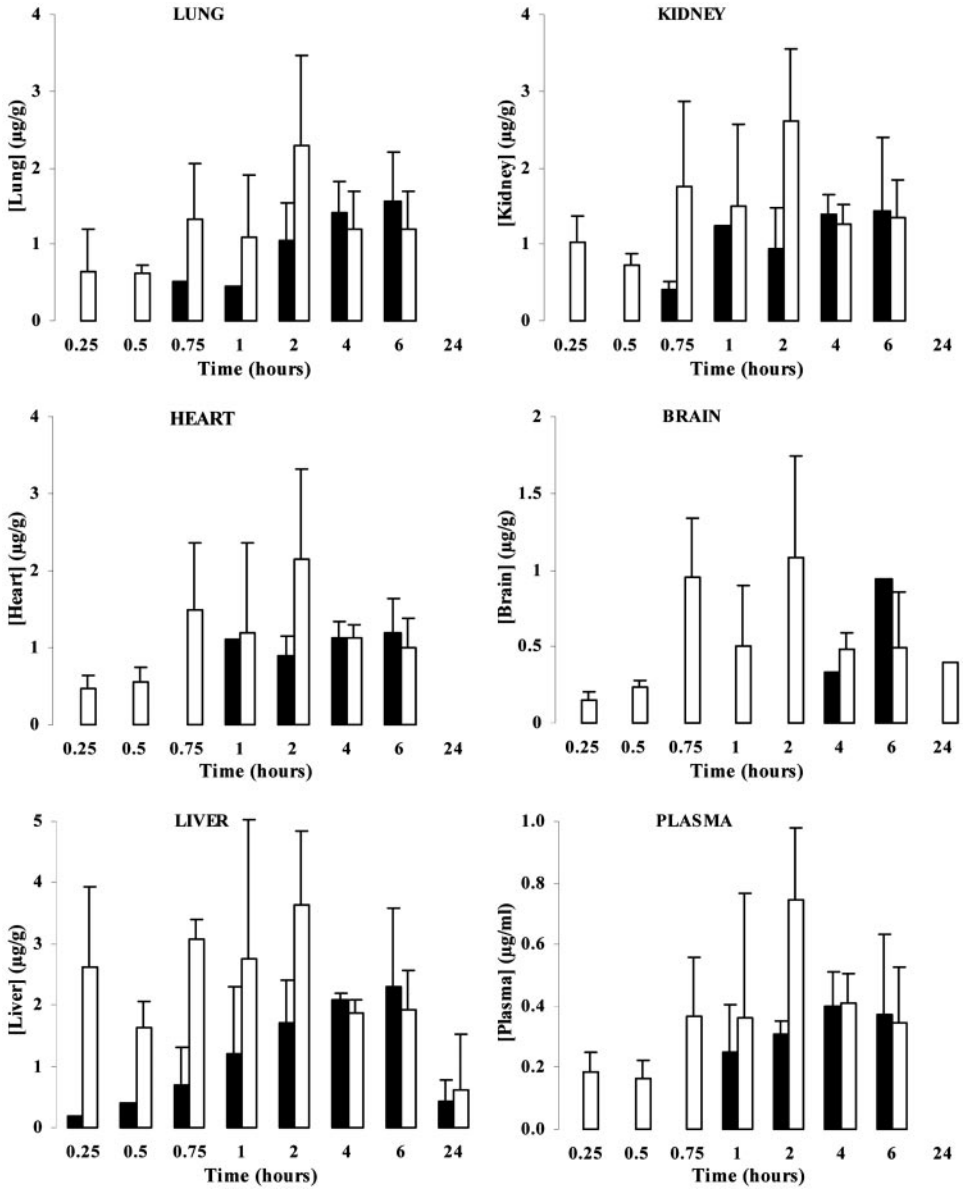

Fig. 3 Concentrations of DIM (□) and LTr_1(■) in plasma and tissues of mice that received I3C (250 mg/kg). Although all mice were sampled, at some time points the levels were below the limit of quantification (100 ng/g tissue, 50 ng/ml plasma). Data show the mean ± SD for three or four mice. Where no *error bars* are shown, measurable amounts were found in one or two of the mice within this group. *DIM*, 3,3′-diindolylmethane; *LTr_1*, [2-(indol-3-ylmethyl)-indol-3-yl] indol-3-ylmethane; *I3C*, indole-3-carbinol.

of HI-IM could tentatively be made (Fig. 5). The estimated concentrations were similar to those of DIM, as were plasma and tissue profiles, reaching maximal concentrations 2 h after administration of I3C. As observed for DIM, HI-IM persisted in the plasma and tissues much longer than I3C, and was still detectable in the liver 24 h after I3C administration.

Disposition of ICZ. ICZ was not detected in the plasma, lung, heart, kidney, or brain. However, a peak with the same retention time as authentic ICZ was detected in the liver of mice 6 and 24 h after I3C administration (Fig. 6). Mass spectral analysis of extracts of combined liver samples afforded the molecular ion of ICZ (*m*/*z* 256), thus providing further evidence that ICZ was present in these samples. The mean concentrations in the liver at 6 and 24 h were 9 and 27 ng/g, respectively.

Plasma Levels and Tissue Distribution of Oxidative Metabolites of I3C. In addition to acid condensation products, oxidative metabolites of I3C were also detected in the plasma. A peak with the same retention time and shape as that of authentic I3CA was detected in plasma samples by HPLC (Fig. 2). The identity of this peak was confirmed by mass spectrometry. I3CA was a significant metabolite, and approximate plasma concentrations were 9.6, 12.6, and 1.1 μg/ml at 15, 30, and 45 min, respectively, after I3C administration. Maximal plasma concentrations of I3CA were 3-fold higher than those of I3C, but as for the parent compound, it was no longer detectable at 1 h after I3C dosing. Although a peak with the retention time of I3CA was also present in tissues of mice that received I3C, it coeluted with the large solvent front, precluding further quantification.

Table 2 Tissue-to-plasma ratios of DIM and LTr_1 in female CD-1 mice that received an oral dose of I3C (250 mg/kg)

Time (h)	Tissue DIM (μg/g)/Plasma DIM (μg/ml)				
	Liver	Kidney	Lung	Heart	Brain
0.25	14.1 ± 5.7	5.6 ± 0.9	3.2 ± 2.1	2.6 ± 0.8	0.9 ± 0.3*
0.5	10.1 ± 2.1	4.7 ± 1.5	3.9 ± 1.0	3.3 ± 0.7	1.5 ± 0.7
0.75	12.1 ± 10.2	4.5 ± 1.0	3.8 ± 1.0	4.0 ± 0.6	2.0 ± 0.6*
1	10.6 ± 6.0	6.7 ± 5.4	3.9 ± 1.8	3.6 ± 1.0	1.3 ± 0.4
2	5.0 ± 1.4	3.5 ± 0.7	3.0 ± 1.2	2.7 ± 1.0	1.3 ± 0.5
4	4.7 ± 1.0	3.1 ± 0.4	3.1 ± 1.8	2.8 ± 0.3	1.2 ± 0.3
6	8.0 ± 7.4	4.7 ± 3.0	4.5 ± 4.0	3.1 ± 0.6	1.4 ± 0.2
	Tissue LTr_1(μg/g)/plasma LTr_1 (μg/ml)				
1	6.8 ± 0.3	nd	nd	nd	nd
2	5.1 ± 2.2	3.3 ± 1.0	3.7 ± 0.6	2.6 ± 0.4	nd
4	7.3 ± 2.7	4.7 ± 1.7	5.3 ± 3.7	3.8 ± 0.9	nd
6	11.1 ± 9.4	4.8 ± 1.5	5.0 ± 0.6	4.1 ± 1.8	nd

NOTE. Results are expressed as mean ± SD of three or four animals; ratios were calculated by taking the plasma and its respective tissue concentration in the same animal.

Abbreviations: DIM, 3,3′-diindolylmethane; LTr_1, [2-(indol-3-ylmethyl)-indol-3-yl] indol-3-ylmethane; nd, not determined as the concentrations in two or more mice in the group at this time point were below the limit of quantification of the analytical method (0.1 μg/g tissue).

* Significant difference ($P < 0.05$) as determined by one-way ANOVA followed by Tukey's post hoc test.

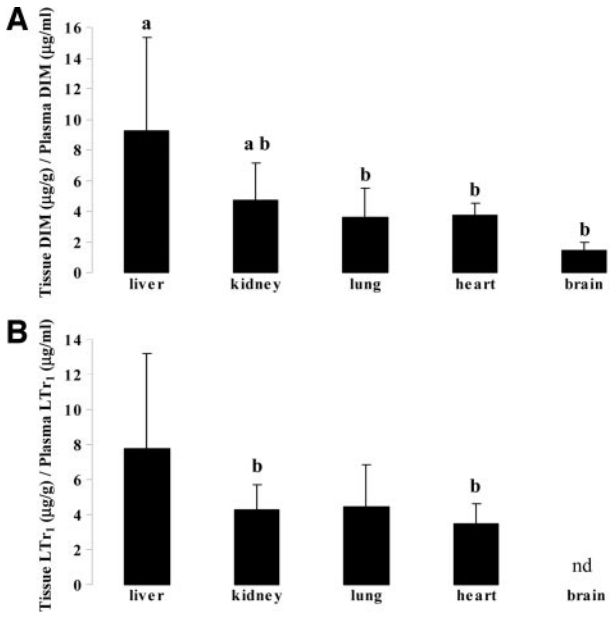

Fig. 4 Mean tissue-to-plasma ratios of (*A*) DIM (*B*) LTr_1 in mice that received I3C by the oral route (250 mg/kg). Data are expressed as mean tissue-to-plasma ratios ± SD. nd, not determined, because the observed concentrations of LTr_1 were (with three exceptions) below the limit of quantification in brain samples; a, significant difference from brain; b, significant difference from liver as determined by one-way ANOVA and Tukey's post hoc test ($P < 0.05$). *DIM*, 3,3′-diindolylmethane; *LTr_1*, [2-(indol-3-ylmethyl)-indol-3-yl] indol-3-ylmethane; *I3C*, indole-3-carbinol.

A second minor oxidative metabolite, I3A was detected in plasma (Fig. 2). Levels were much lower than those of I3CA. By combining HPLC fractions of the peak of interest, confirmation of its identity was possible using mass spectrometry. Accurate quantification of I3A in plasma was difficult, with levels being at the limit of detection. However, maximal peak levels at 30 min after I3C administration gave peak area ratios approximately equal to 50 ng/ml of a spiked I3A standard. Again, levels were undetectable 1 h after dosing. I3A was not detectable in tissues.

DISCUSSION

This study characterizes the fate of I3C and quantifies the parent compound and its acid condensation products in the plasma, liver, kidney, lung, heart, and brain of mice that received I3C by the oral route. It is the first study to accurately quantify I3C, DIM, LTr_1, and ICZ using standards for the individual compounds and a fully validated analytical assay. By allometric scaling, 250 mg/kg in mice is equivalent to a dose of 20 mg/kg in an average adult human, significantly more than would be ingested in the diet. It is therefore important to

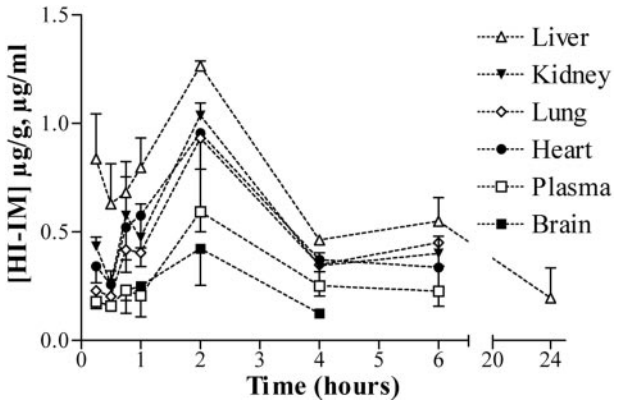

Fig. 5 Estimated plasma and tissue concentrations of HI-IM in mice that received I3C by the oral route (250 mg/kg). Data points show the mean and SE in one direction ($n = 4$). *HI-IM*, 1-(3-hydroxymethyl)-indolyl-3-indolylmethane; *I3C*, indole-3-carbinol.

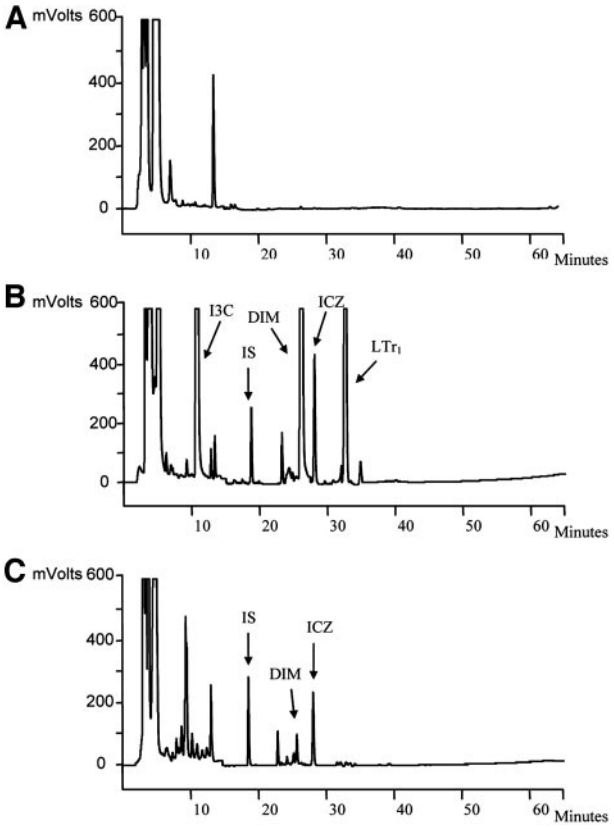

Fig. 6 High-performance liquid chromatography chromatograms of (*A*) liver samples from control mice (*B*) control liver samples spiked with a mixture containing ICZ, DIM, I3C, IS, and LTr_1 and (*C*) liver samples from mice, 24 h after a single oral administration of I3C (250 mg/kg). ICZ was the only product quantified using fluorescence detection at 335:415 nm (ex./em). *ICZ*, indolo [3,2b]carbazole; *DIM*, 3,3′-diindolylmethane; *I3C*, indole-3-carbinol; *IS*, internal standard; *LTr_1*, [2-(indol-3-ylmethyl)-indol-3-yl] indol-3-ylmethane.

consider that the disposition of I3C may be dose-related, such that the relative levels of metabonates and their tissue distribution at dietary levels, or after the administration of agents in tablet form, could be different from the results obtained in this study.

Oral administration of I3C to mice resulted in the detection of parent compound in plasma and tissues. In general, maximal I3C concentrations observed were considerably higher than those for its acid condensation products ([I3C] > [DIM] > [LTr_1] > [HI-IM] ⋙ [ICZ]). This is in contrast with investigations reported previously in a number of species, where condensation products of I3C were detected, but not I3C itself (18, 26, 28, 29). Our first sampling time point was 15 min, earlier than those used in previous studies. Rapid absorption and elimination of I3C was evident, possibly explaining why the presence of I3C in plasma may have been missed by others.

Additionally, oligomerization of I3C is dependent on pH (16, 29). Because humans have a fasting gastric acid pH of 1.5–2.0 (30), leading to more rapid acid-catalyzed oligomerization of I3C than the pH of 3.5–4.0 found in this study with fed mice, this may be one explanation why I3C has been undetectable in human studies (26). However, the fasting pH in mice is also around 1.5 (31), whereas in humans the gastric pH rises after a meal, suggesting that oligomerization in the two species may be similar. Finally, I3C readily underwent oligomerization during extraction from plasma, if the method was not chosen carefully (17). This instability may also contribute to the lack of detection of I3C in plasma.

In vitro and *in vivo* studies demonstrate that I3C is a pharmacologically active compound (12–14, 32). However, some *in vivo* studies show I3C to be effective only when administered orally and not by the i.p. route (9, 33). DIM and LTr_1 have been proven to have potential antitumor activity in their own right (22, 34, 35), and detection of these compounds *in vivo* suggests that they could indeed be partially responsible for some of the observed activity of orally administered I3C. The biological activity of HI-IM has not been reported to date.

The detection of significant quantities of I3C itself suggests that the parent compound could be partly responsible for any pharmacological effect observed *in vivo*. At the earliest sampling time point of 15 min, plasma and tissue concentrations had already reached an apparent maximum. Thus, the possibility exists that concentrations of I3C were even higher immediately before or after sampling at 15 min.

Not only was it the case that acid condensation products of I3C (*i.e.* DIM, LTr_1, and HI-IM) were detected in plasma and tissues at lower peak concentrations than I3C itself, but these levels were not reached until 2 (DIM; HI-IM) and 6 (LTr_1) h after I3C dosing. However, DIM, LTr_1, and HI-IM persisted in plasma and tissues much longer than I3C (Table 1; Figs. 3 and 5). Because formation of acid condensation products is rapid at acidic gut pH (29), the time taken for achievement of peak levels of DIM, LTr_1, and HI-IM is most likely a characteristic of the time taken for the systemic absorption of these compounds once formed within the stomach.

All of the tissues sampled in this study (*i.e.*, liver, kidney, brain, heart, and lung) are well-perfused organs, and it follows that all compounds should reach these tissues rapidly after absorption into the systemic circulation. Indeed, high peak concentrations of I3C were observed in tissues during the first few minutes after absorption, and tissue concentration profiles of all compounds followed the same pattern as those for plasma, indicating a rapid equilibrium of all compounds between tissue and plasma. I3C, DIM, LTr_1, and HI-IM were detected in all of the tissues investigated. However, concentrations of all compounds were lowest in the brain and LTr_1 was detected in this tissue in only 3 of the 32 mice studied (4 and 6 h after I3C administration) making it impossible to calculate accurate tissue-to-plasma ratios. It is possible that these compounds are subject to efflux transport at the blood-brain barrier, being substrates for P-glycoprotein for example (36), thus limiting brain tissue exposure. Regarding LTr_1, it is possible that the relatively high limit of detection of the analytical assay precludes its measurement in brain. Levels of I3C and its oligomers were generally higher in tissues than in plasma, possibly attributable to the lipid solubility of the compounds, but distribution was rapid, and there was no apparent sequestration/accumulation (Fig. 4). If binding of I3C and its condensation products to tissue constituents occurs, it appears to be highly reversible. Concentrations of all compounds were highest in the liver. This

organ, which represents a fairly large fraction of body mass, appears to act as a sizeable reservoir for I3C and related compounds. Detection of HI-IM, DIM, and LTr_1 in the liver, after oral administration of I3C, is consistent with observations of other investigators who identified these condensation products in the liver of rats (18, 28, 29) that received I3C. LTr_1 has also been identified in the liver of rat pups from I3C-fed dams (28).

From the data presented in Table 2, it is evident that DIM and LTr_1 tissue-to-plasma concentration ratios are comparable, although actual concentrations of DIM were higher than those for LTr_1 (Fig. 3). First, this may reflect the relative amounts of each compound formed from I3C in the gut, where kinetic probability indicates that formation of a dimer will occur more easily than formation of a trimer. Second, the finding indicates differences between DIM and LTr_1 in the rate and extent of absorption.

It is known that ICZ is a potent inducer of cytochrome P450 enzymes *in vivo*. It has been shown *in vitro* to bind with high affinity to the Ah receptor (37) and transcriptionally activate the *CYP1A1* gene (38). Taking into account the variation in I3C dosage between studies, the levels of ICZ in the liver reported in this study are higher than those reported previously (18, 39). However, neither of these groups fully validated their analytical method, and without taking factors such as extraction efficiency into account, it is difficult to assess absolute concentrations.

I3CA was a major oxidative metabolite of I3C in plasma samples, in agreement with unpublished data in Wall *et al.* (40). I3A was detected at very low levels in the plasma up to and including 45 min. This finding is also consistent with previous studies, where I3A was found to be an oxidative product of I3C (unpublished results in Ref. 41). It is possible that formation of these oxidative products from I3C could contribute to its rapid clearance from plasma. I3CA and I3A are themselves rapidly formed and cleared within the 1st h of I3C administration.

I3CA and I3A appear to be detoxification products of I3C. These oxidative compounds have been identified *in vitro* in human breast tumor cells treated with I3C but also in the absence of cells, indicating that enzyme activity is not required for their formation (42). It is unknown whether this oxidative process can also be enzyme catalyzed *in vivo*. I3CA and I3A do not exhibit the same free radical scavenging activity as I3C (43). A study by Gamet-Payrastre *et al.* (44) showed that I3C and DIM significantly inhibited the growth of human colon adenocarcinoma (HT29) cells but that I3CA, at the same concentration of 100 μM, did not significantly affect cell viability. Recent work by Staub *et al.* (42) found I3A to be less active than I3C in cell growth and cell cycle assays, with no effect on CDK6 expression as has been reported for I3C (12).

In conclusion, this is the most comprehensive study of the fate of I3C *in vivo* to date. I3C, DIM, LTr_1, and HI-IM have all been shown to be present in significant levels in plasma and a number of well-perfused tissues, after administration of I3C. ICZ did not appear to be present in significant concentrations. Although there have been a few studies on the disposition of I3C in a range of species (18, 25, 26, 29, 45), most of them used radiolabeled I3C (18, 25, 45) and none fully addressed the fate of I3C *per se*. This study has highlighted the importance of examining earlier time points in investigating the pharmacology of this potential chemopreventive agent and will aid the interpretation of studies investigating the *in vivo* activity of orally administered I3C.

REFERENCES

1. Verhoeven DTH, Goldbohm RA, van Poppel G, Verhagen H, van den Brandt PA. Epidemiological studies on brassica vegetables and cancer risk. Cancer Epidemiol Biomark Prev 1996;5:733–48.

2. Verhoeven DTH, Verhagen H, Goldbohm RA, van den Brandt PA, van Poppel G. A review of mechanisms underlying anticarcinogenicity by brassica vegetables. Chem Biol Interact 1997;103:79–129.

3. Bradlow HL, Michnovicz J, Telang NT, Osborne MP. Effects of dietary indole-3-carbinol on estradiol metabolism and spontaneous mammary tumors in mice. Carcinogenesis (Lond) 1991;12:1571–4.

4. Grubbs CJ, Steele VE, Casebolt T, et al. Chemoprevention of chemically-induced mammary carcinogenesis by indole-3-carbinol. Anticancer Res 1995;15:709–16.

5. Manson MM, Hudson EA, Ball HW, et al. Chemoprevention of aflatoxin B1-induced carcinogenesis by indole-3-carbinol in rat liver–predicting the outcome using early biomarkers. Carcinogenesis (Lond) 1998;19:1829–36.

6. Morse MA, Lagreca SD, Amin SG, Chung FL. Effects of indole-3-carbinol on lung tumorigenesis and DNA methylation induced by 4-(methylnitrosamino)-1-(3-pyridyl)-1-butanone (Nnk) and on the metabolism and disposition of Nnk in A/J mice. Cancer Res 1990;50:2613–7.

7. Tanaka T, Kojima T, Morishita Y, Mori H. Inhibitory effects of the natural products indole-3-carbinol and sinigrin during initiation and promotion phases of 4-nitroquinoline 1-oxide-induced rat tongue carcinogenesis. Jpn J Cancer Res 1992;83:835–42.

8. Kojima T, Tanaka T, Mori H. Chemoprevention of spontaneous endometrial cancer in female Donryu rats by dietary indole-3-carbinol. Cancer Res 1994;54:1446–9.

9. Bradfield CA, Bjeldanes LF. Effect of dietary indole-3-carbinol on intestinal and hepatic monooxygenase, glutathione S-transferase and epoxide hydrolase activities in the rat. Food Chem Toxicol 1984;22:977–82.

10. Manson MM, Ball HWL, Barrett MC, et al. Mechanism of action of dietary chemoprotective agents in rat liver: induction of phase I and II drug metabolizing enzymes and aflatoxin B-1 metabolism. Carcinogenesis (Lond) 1997;18:1729–38.

11. Michnovicz JJ, Bradlow HL. Altered estrogen metabolism and excretion in humans following consumption of indole-3-carbinol. Nutr Cancer 1991;16:59–66.

12. Cover CM, Hsieh SJ, Tran SH, et al. Indole-3-carbinol inhibits the expression of cyclin-dependent kinase-6 and induces a G1 cell cycle arrest of human breast cancer cells independent of estrogen receptor signaling. J Biol Chem 1998;273:3838–47.

13. Howells LM, Gallacher-Horley B, Houghton CE, Manson MM, Hudson EA. Indole-3-carbinol inhibits protein kinase B/Akt and induces apoptosis in the human breast tumor cell line MDA MB468 but not in the nontumorigenic HBL100 line. Mol Cancer Ther 2002;1:1161–72.

14. Chinni SR, Li YW, Upadhyay S, Koppolu PK, Sarkar FH. Indole3-carbinol (I3C) induced cell growth inhibition, G1 cell cycle arrest and apoptosis in prostate cancer cells. Oncogene 2001;20:2927–36.

15. Chinni SR, Sarkar FH. Akt inactivation is a key event in indole-3-carbinol-induced apoptosis in PC-3 cells. Clin Cancer Res 2002;8:1228–36.

16. Grose KR, Bjeldanes LF. Oligomerization of indole-3-carbinol in aqueous acid. Chem Res Toxicol 1992;5:188–93.

17. Anderton MJ, Jukes R, Lamb JH, et al. Liquid chromatographic assay for the simultaneous determination of indole-3-carbinol and its acid condensation products in plasma. J Chromatogr B 2003;787:281–91.

18. Stresser DM, Williams DE, Griffin DA, Bailey GS. Mechanisms of tumor modulation by indole-3-carbinol. Disposition and excretion in male Fischer 344 rats. Drug Metab Dispos 1995;23:965–75.

19. Riby JE, Feng C, Chang YC, Schaldach CM, Firestone GL, Bjeldanes LF. The major cyclic trimeric product of indole-3-carbinol is a strong agonist of the estrogen receptor signaling pathway. Biochemistry 2000;39:910–8.

20. Bjeldanes LF, Kim JY, Grose KR, Bartholomew JC, Bradfield CA. Aromatic hydrocarbon responsiveness-receptor agonists generated from indole-3-carbinol in vitro and in vivo: comparisons with 2,3,7,8-tetrachlorodibenzo-p-dioxin. Proc Natl Acad Sci USA 1991;88:9543–7.

21. Chang YC, Riby J, Chang GH, Peng BC, Firestone G, Bjeldanes LF. Cytostatic and antiestrogenic effects of 2-(indol-3-ylmethyl)-3,3′-diindolylmethane, a major in vivo product of dietary indole-3-carbinol. Biochem Pharmacol 1999;58:825–34.

22. Hong CB, Kim HA, Firestone GL, Bjeldanes LF. 3,3′-Diindolylmethane (DIM) induces a G(1) cell cycle arrest in human breast cancer cells that is accompanied by Sp1-mediated activation of p21(WAF1/CIP1) expression. Carcinogenesis (Lond) 2002;23:1297–305.

23. Chen I, McDougal A, Wang F, Safe S. Aryl hydrocarbon receptor-mediated antiestrogenic and antitumorigenic activity of diindolylmethane. Carcinogenesis (Lond) 1998;19:1631–9.

24. IARC Handbooks of Cancer Prevention. Cruciferous vegetables, isothiocyanates and indoles. IARC Press, Lyon. In press 2004.

25. Dashwood RH, Uyetake L, Fong AT, Hendricks JD, Bailey GS. In vivo disposition of the natural anti-carcinogen indole-3-carbinol after po administration to rainbow trout. Food Chem Toxicol 1989;27:385–92.

26. Arneson DW, Hurwitz A, McMahon LM, Robaugh D. Presence of 3,3′-diindolylmethane in human plasma after oral administration of indole-3-carbinol [abstract 2833]. Proc Am Assoc Cancer Res 1999;40:429.

27. Pindur U, Muller J. Indolo[3,2-B]carbazole–product of the reaction of 3,3′- bisindolylmethane with triethyl orthoformate. Archiv der Pharmazie 1987;320:280–2.

28. Larsen-Su SA, Williams DE. Transplacental exposure to indole-3-carbinol induces sex-specific expression of CYP1A1 and CYP1B1 in the liver of Fischer 344 neonatal rats. Toxicol Sci 2001;64:162–8.

29. De Kruif CA, Marsman JW, Venekamp JC, et al. Structure elucidation of acid reaction products of indole-3-carbinol: detection in vivo and enzyme induction in vitro. Chem Biol Interact 1991;80:303–15.

30. Washington N, Washington C, Wilson CG, editors. The stomach. In: Physiological pharmaceutics, biological barriers to drug absorption. London: Taylor and Francis; 2000. p. 75–103.

31. Helander HF. Gastric acidity in young and adult mice. Scand J Gastroenterol 1969;5:221–4.

32. Srivastava BH, Shukla Y. Antitumour promoting activity of indole-3-carbinol in mouse skin carcinogenesis. Cancer Lett 1998;134:91–5.

33. Park JY, Bjeldanes LF. Organ-selective induction of cytochrome P-450-dependent activities by indole-3-carbinol-derived products: influence on covalent binding of benzo[a]pyrene to hepatic and pulmonary DNA in the rat. Chem Biol Interact 1992;83:235–47.

34. Leong H, Firestone GL, Bjeldanes LF. Cytostatic effects of 3,3′-diindolylmethane in human endometrial cancer cells result from an estrogen receptor-mediated increase in transforming growth factor-alpha expression. Carcinogenesis (Lond) 2001;22:1809–17.

35. Christensen JG, LeBlanc GA. Reversal of multidrug resistance in vivo by dietary administration of the phytochemical indole-3-carbinol. Cancer Res 1996;56:574–81.

36. Stauch TR, Gudmundsson O. Progress in understanding the structure-activity relationships of P-glycoprotein. Adv Drug Delivery Rev 2002;54:315–28.

37. Gillner M, Bergman J, Cambillau C, Fernstrom B, Gustafsson JA. Interactions of indoles with specific binding sites for 2,3,7,8-tetrachlorodibenzo-p-dioxin in rat liver. Mol Pharmacol 1985;28:357–63.

38. Kleman MI, Poellinger L, Gustafsson JA. Regulation of human dioxin receptor function by indolocarbazoles, receptor ligands of dietary origin. J Biol Chem 1994;269:5137–44.

39. Kwon CS, Grose KR, Riby J, Chen YH, Bjeldanes LF. In-vivo production and enzyme-inducing activity of indole[3,2-B] carbazole. J Agric Food Chem 1994;42:2536–40.

40. Wall ME, Taylor H, Perera P, Wani MC. Indoles in edible members of the Cruciferae. J Nat Prod 1988;51:129–35.

41. Wortelboer HM, van der Linden EC, de Kruif CA, et al. Effects of indole-3-carbinol on biotransformation enzymes in the rat: in vivo changes in liver and small intestinal mucosa in comparison with primary hepatocyte cultures. Food Chem Toxicol 1992;30:589–99.

42. Staub RE, Feng C, Onisko B, Bailey GS, Firestone GL, Bjeldanes LF. Fate of indole-3-carbinol in cultured human breast tumor cells. Chem Res Toxicol 2002;15:101–9.

43. Arnao MB, Sanchez-Bravo J, Acosta M. Indole-3-carbinol as a scavenger of free radicals. Biochem Mol Biol Int 1996;39:1125–34.

44. Gamet-Payrastre L, Lumeau S, Gasc N, Cassar G, Rollin P, Tulliez J. Selective cytostatic and cytotoxic effects of glucosinolate hydrolysis products on human colon cancer cells in vitro. Anticancer Drugs 1998;9:141–8.

45. Shertzer HG, Berger ML, Tabor MW. Intervention in free radical mediated hepatotoxicity and lipid peroxidation by indole-3-carbinol. Biochem Pharmacol 1988;37:333–8.